Hydroxy-cruciforms†

Psaras L. McGrier,[a] Kyril M. Solntsev,[a] Jan Schönhaber,[b] Scott M. Brombosz,[a] Laren M. Tolbert[a] and Uwe H. F. Bunz*[a]

The synthesis of hydroxy-cruciforms 7 and 8 and their dramatically varying photophysical properties upon exposure to amines are reported.

Cruciform fluorophores (tetra-1,2,4,5-vinyl- or -ethynyl-substituted benzenes, XFs) are π-systems with unusual frontier molecular orbitals (FMOs). If one of the axes is donor substituted and the other axis is acceptor substituted, species with *spatially separated* FMOs can result. The HOMO is localized on the donor part of the molecule, while the LUMO is localized on the acceptor part of the molecule. This FMO arrangement leads to a situation in which electronic information can be addressed spatially and for which HOMO and LUMO are manipulated by metal cations or by protons. We[1] and others[2–5] have shown that dialkylaniline- and pyridine-containing XFs display unusually large bathochromic or hypsochromic shifts when exposed to zinc, magnesium, calcium and manganese salts or protons.[1,2] The reason for the large shifts in absorption and emission is the independently addressable HOMO and LUMO, enforcing large changes in the HOMO–LUMO gap.[3] Up to now, HOMO–LUMO of XF-types have been addressed by cationic species, binding to the free electron pairs of pyridines and dialkylanilines. In this contribution we demonstrate that XFs carrying strategically placed phenol functionalities show unusual photophysical effects upon deprotonation and exposure to amines.

The synthesis of hydroxy-XFs starts with the reaction of phosphonate 1[6] with either the protected aldehyde 2 or 3 to give the distyrylbenzene derivatives 4 and 5 in 77% and 68% yield, respectively, after chromatography and crystallization. Coupling of 4 or 5 with 4-*tert*-butylphenylacetylene in the presence of CuI–(Ph3P)2PdCl2 under standard Heck–Cassar–Sonogashira–Hagihara conditions[7] in piperidine furnished the target XFs 7 and 8, after aqueous workup, chromatography and subsequent deprotection with trifluoroacetic acid at −78 °C in dichloromethane, as yellow or yellowish–brown solids in 41% and 40% yield respectively (Scheme 1). The relatively low coupling yield (44 and 48% respectively) is due to losses during the chromatography of the intermediate. Nevertheless, the target XFs are easily available on a 100–200 mg scale. If 4 is coupled to 9, we obtain an intermediate in 53% yield, which is deprotected in 85% yield to give 10.

[a] School of Chemistry and Biochemistry, Georgia Institute of Technology, Atlanta, GA 30332, USA.
E-mail: uwe.bunz@chemistry.gatech.edu
[b] Institut für Organische Chemie, Universität Heidelberg, Im Neuenheimer Feld 270, D-69120 Heidelberg, FRG
† Electronic supplementary information (ESI) available: Experimental and spectral data. See DOI: 10.1039/b702883k
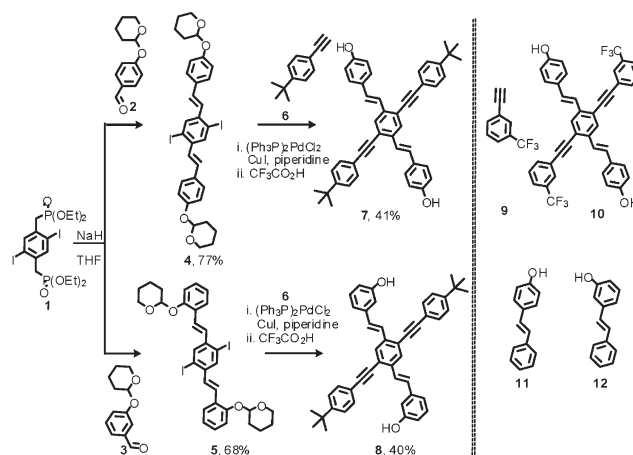
Scheme 1 Synthesis of hydroxy-XFs 7 and 8.

Table 1 shows the pertinent photophysical data of 7, 8 and 10. The XFs 7 and 8 are similar to each other, as they show blue emission with robust quantum yields. Attachment of –CF3 groups on the aryleneethynylene axis in 10 decreases the band gap and leads to significantly red-shifted absorption and emission. The Stokes shifts in these XFs are similar and around 3000 cm^{-1}. The vibronic progression of 8 is in the expected range, while that of 7 is smaller. The fluorescence spectrum of 10 does not show any vibronic bands, suggesting that its excited state is structurally different from its ground state.[8]

We titrated (Figs. 1, 2) 7 and 8 in a methanol–water mixture with aqueous base (KOH). Fig. 1 shows absorption and emission for 8. Upon addition of hydroxide *there is no significant change in the absorption spectrum of 8*; the emission of the phenolate of 8 is largely quenched. A very weak emission band for the deprotonated form of 8 is observed at 515 nm. The invariance of the absorption spectrum is surprising and persists upon addition of a large excess of hydroxide. In the case of 7, upon deprotonation (Fig. 2), the absorption spectrum shows an appreciable red shift, as would be expected for a phenolate, with a prominent absorption appearing

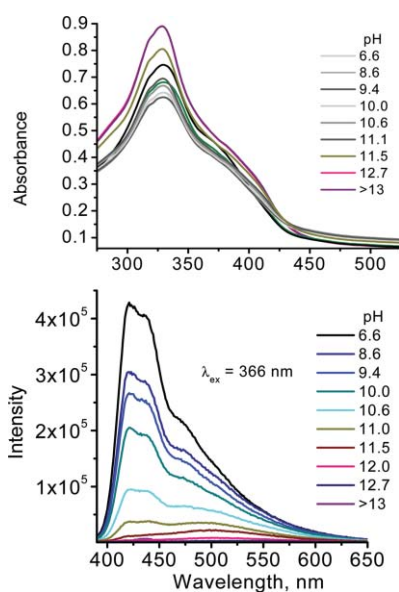**Table 1** Photophysical data of 7, 8 and 10 in dichloromethane solution

CH$_2$Cl$_2$	7	8	10
Absorption (nm)	380	376	404
Emission (nm)	432	423	456
Vibronic progression (cm^{-1})	876	1219	none
Stokes shift (cm^{-1})	3167	2955	2822
Φ	0.41	0.72	0.57
τ (ns)	1.42	2.99	na

Fig. 1 Uv–Vis (top) and emission (bottom) spectra of XF **8** in a 2 : 1 vol. methanol–water mixture at different pH-values.

at 416 nm. At the same time, the emission changes from 476 nm (blue) to 580 nm (yellow). Addition of an excess of KOH solution does not change the emission wavelength further. From the titrations, the pK_a values for **7** and **8** were determined to be 9.9 and 10.0.

Changes in spectroscopic properties are not only observed upon deprotonation of the XFs **7** and **8** in methanol–water mixtures but also when solutions of XFs in dichloromethane are exposed to amines. Fig. 3 shows a photograph of the XFs **7**, **8** and **10** exposed to a panel of different amines, ordered by their increasing pK_a values, while Fig. 4 (bottom) shows the corresponding emission spectra.
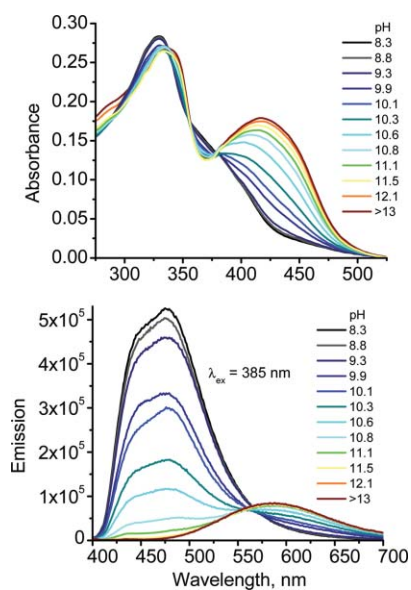
Fig. 2 Uv–Vis (top, 417 nm λ_{max} deprotonated form) and emission (bottom 474 nm, 596 nm λ_{max}) spectra of XF **7** in a 2 : 1 vol. methanol–water mixture at different pH-values.
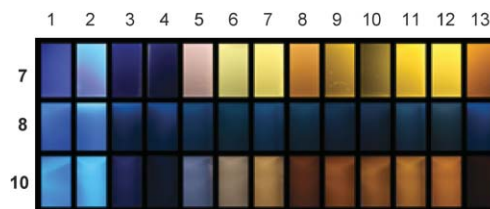
Fig. 3 Photograph of the XFs **7**, **8**, and **10**: 1) reference; exposure to 2) pyrrole (–), 3) quinoline (4.90), 4) pyridine (5.25), 5) imidazole (6.96; $\lambda_{max.7}$ = 551 nm), 6) morpholine (8.33; 555 nm), 7) piperazine (9.83; 556 nm), 8) ethylene diamine (10.7; 579 nm), 9) piperidine (10.8; 564 nm), 10) triethylamine (10.8; 555 nm), 11) diethylamine (11.0; 562 nm), 12) diisopropylamine (11.1; 558 nm), and 13) 1,8-diazabicyclo[5.4.0]undec-7-ene (DBU, ~12; 572 nm). The numbers in parentheses are the pK_a values of the corresponding ammonium ions. The photographs are taken in 15 mL vials under a hand held black light (λ_{max} = 366 nm).
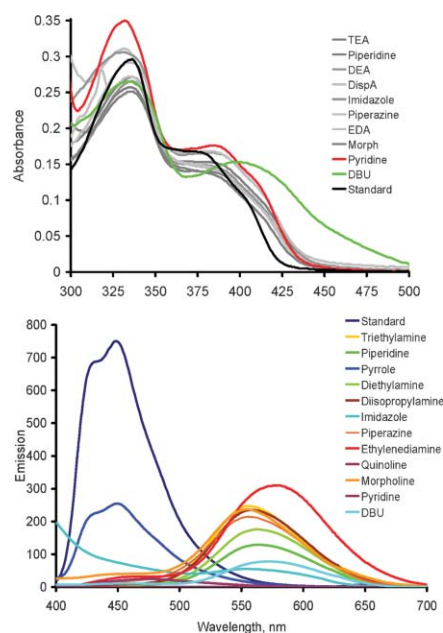
Fig. 4 Absorption spectra (top) of solutions of **7** in DCM upon addition of amine (0.1 mL). Emission spectra (bottom) of solutions of **7** in dichloromethane (DCM, 15 mL, vial) upon addition of amine (0.1 mL).

Interestingly, the magnitude in shift and the pK_a-values of the amines do not correlate particularly well, as ethylenediamine (pK_a = 10.7), *i.e.* not the most basic amine, displays the largest red shift. In the case of the exposure of **7** to quinoline or to pyridine, fluorescence is quenched, possibly due to a back electron transfer following proton transfer to the basic nitrogen.[9] If the amine under consideration is not very basic, as pyrrole and imidazole, either there is no change of the emission or a mixed color (imidazole) is observed. Similar trends are observed for XF **10**, even though the emission intensities are much lower, as is expected from the energy gap law.[10]

Exposure of the XF **8** to amines in dichloromethane results in quenching (see SI for spectra) of the emission, similar to that observed on exposure of **8** to KOH. The above observations demonstrate that **7** and **8** are different from hydroxystilbenes **11** and **12**. The phenolate of stilbene **11** is weakly fluorescent, while that of the *meta*-compound **12** is quite fluorescent.[11] In **11** and **12**

the excited state acidity of the phenolic function is significantly enhanced, that of **12** more so than that of **11**. Neither the XF **7** nor **8**, on the other hand, shows dramatically enhanced photoacidity in methanol–water mixtures with up to 50% vol. water,[11] which makes them comparable to the weak photoacid 2-naphthol with a pK_a* of 2.8.[12]

The absorption and emission spectra of **7** show a more complex behavior in the presence of amines (Fig. 4). On the one hand, except for 1,8-diaza[5.4.0]bicycloundecene (DBU, pK_a ∼ 12), the absorption maxima show a shift of *ca.* 20 nm and are consistent with a hydrogen-bonded complex.[13] Upon addition of DBU a red-shifted feature is observed, which we attribute to the fully bis-deprotonated ground state species, as it is identical to that observed in the KOH-promoted deprotonation of **7**. On the other hand, all of the amine complexes exhibit efficient emission from the fully deprotonated (ion pair) state. From these observations we conclude that in dichloromethane solutions the difference in pK_a (or ΔG of the proton transfer) between **7*** and amines is sufficient to produce solvent-separated ion pairs.[14] In the ground state, the observed ΔpK_a results in the formation of hydrogen-bonded complexes.

The observation of different, amine-dependent emission characteristics is of potential importance since Lavigne *et al.*[15] have shown that carboxylate-substituted polythiophenes can discern biogenic amines when the absorption spectra of the complexes are compared. Our approach is complementary as we use more sensitive fluorescence spectroscopy.

What is the reason for the dramatic differences in the optical properties of **7** and **8** upon interaction with bases, *i.e.* proton-dissociation induced red shift *vs.* quenching? A DFT calculation (Fig. 5) of the FMO-distribution of **7** and **8** sheds light on this issue. In the dianion of **7**, HOMO and LUMO show spatial overlap in the central ring and both absorption and emission are Franck–Condon allowed. In the case of **8** the situation is different. Due to the disjoint orbital structure *in which the HOMO is localized only on the two phenolate rings, while the LUMO is strictly localized on the bisarylethynyl axis, there is a vanishingly small spatial overlap between the two frontier molecular orbitals, resulting in a Franck–Condon forbidden transition. Without the quantum chemical calculations, the different spectroscopic properties of 7^{2-} and 8^{2-} would be very hard to rationalize.* Since the 340 nm transition is both invariant with respect to deprotonation and strongly allowed, we conclude that this is a HOMO–LUMO transition in **8** but a HOMO–LUMO + n-transition in the deprotonated form of **8**, while the weaker HOMO–LUMO transition of the dianion of **8** is hidden in the baseline.[3] The allowed transition in the dianion must have a similar gap to the HOMO–LUMO-transition in the neutral compound, explaining the lack of change in the absorption spectra.

In conclusion, we have prepared the two XFs **7** and **8** and investigated their photophysical properties upon deprotonation or exposure to amines. We see dramatic differences between the *para* (**7**) and the *meta* (**8**) XF as a consequence of the different FMO distribution. The dianion **8** suffers from a Franck–Condon disallowed HOMO–LUMO-transition, which is responsible for the observed fluorescence quenching. Potential applications of such materials with separated FMOs include exciton collection and splitting in photovoltaic devices and fluorescence sensors in cases where the XFs are equipped with additional binding elements.
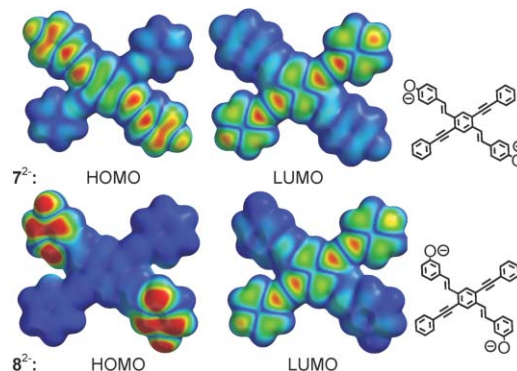
Fig. 5 Density of the frontier molecular orbitals (HOMO and LUMO) of the bisphenolate anions of models of **7** and of **8** (*tert*-butyl groups are omitted) as calculated by B3LYP-6-31G**//B3LYP-6-31G** using SPARTAN.

Notes and references

1 J. N. Wilson and U. H. F. Bunz, *J. Am. Chem. Soc.*, 2005, **127**, 4124–4125; J. N. Wilson, M. Josowicz, Y. Q. Wang and U. H. F. Bunz, *Chem. Commun.*, 2003, 2962–2963; A. J. Zucchero, J. N. Wilson and U. H. F. Bunz, *J. Am. Chem. Soc.*, 2006, **128**, 11872–11881; W. W. Gerhardt, A. J. Zucchero, J. N. Wilson, C. R. South, U. H. F. Bunz and M. Weck, *Chem. Commun.*, 2006, 2141–2142.

2 E. L. Spiteler, L. D. Shirtlcliff and M. M. Haley, *J. Org. Chem.*, 2007, **72**, 86–96; J. A. Marsden, J. J. Miller, L. D. Shirtcliff and M. M. Haley, *J. Am. Chem. Soc.*, 2005, **127**, 2464–2476.

3 A. Zen, A. Bilge, F. Galbrecht, R. Alle, K. Meerholz, J. Grenzer, D. Neher, U. Scherf and T. Farrell, *J. Am. Chem. Soc.*, 2006, **128**, 3914–3915; A. L. Thompson, T. S. Ahn, K. R. J. Thomas, S. Thayumanavan, T. J. Martinez and C. J. Bardeen, *J. Am. Chem. Soc.*, 2005, **125**, 16348–16349; H. Meier, B. Mühling and H. Kolshorn, *Eur. J. Org. Chem.*, 2004, 1033–1042.

4 H. Kang, G. Evmenenko, P. Dutta, K. Clays, K. Song and T. J. Marks, *J. Am. Chem. Soc.*, 2006, **128**, 6194–6205; K. Hu, P. W. Zhu, Y. Yu, A. Facchetti and T. J. Marks, *J. Am. Chem. Soc.*, 2004, **126**, 15974–15975.

5 J. K. Sorensen, M. Vestergaard, A. Kadziola, K. Kilsa and M. B. Nielsen, *Org. Lett.*, 2006, **8**, 1173–1176.

6 J. N. Wilson, P. M. Windscheif, U. Evans, M. L. Myrick and U. H. F. Bunz, *Macromolecules*, 2002, **35**, 8681–8683.

7 U. H. F. Bunz, *Chem. Rev.*, 2000, **100**, 1605–1644; K. Sonogashira, *J. Organomet. Chem.*, 2002, **653**, 46–49; E. Negishi and L. Anastasia, *Chem. Rev.*, 2003, **103**, 1979–2017.

8 J. S. Yang, S. Y. Chiou and K. L. Liau, *J. Am. Chem. Soc.*, 2002, **124**, 2518–2527.

9 Q. Zhou and T. M. Swager, *J. Am. Chem. Soc.*, 1995, **117**, 12593–12602; J. G. Müller, E. Atas, C. Tan, K. S. Schanze and V. D. Kleiman, *J. Am. Chem. Soc.*, 2006, **128**, 4007–4016.

10 J. V. Caspar and T. J. Meyer, *J. Phys. Chem.*, 1983, **87**, 952–957; L. M. Tolbert, S. M. Nesselroth, T. L. Netzel, N. Raya and M. Stapleton, *J. Phys. Chem.*, 1992, **96**, 4492–4496.

11 F. D. Lewis and E. M. Crompton, *J. Am. Chem. Soc.*, 2003, **125**, 4044–4045; F. D. Lewis, L. E. Sinks, W. Weigel, M. C. Sajimon and E. M. Crompton, *J. Phys. Chem. A*, 2005, **109**, 2443–2451.

12 L. M. Tolbert and K. M. Solntsev, *Acc. Chem. Res.*, 2002, **35**, 19–27.

13 H. Baba and S. J. Suzuki, *Chem. Phys.*, 1961, **35**, 1118–1127.

14 N. K. Zaitsev, A. B. Demyashkevich and M. G. Kuzmin, *High Energy Chem.*, 1980, **14**, 116–120.

15 T. L. Nelson, C. O'Sullivan, N. T. Greene, M. S. Maynor and J. J. Lavigne, *J. Am. Chem. Soc.*, 2006, **128**, 5640–5641.